Electronic Supplementary Material (ESI) for RSC Advances.

Supporting Information

On the Role of Metal Atoms Doping in Hematite for Improved Photoelectrochemical Properties: a Comparison Study

Jinzhan Su,* Jian Wang, Cong Liu, Bo Feng, Yubin Chen, Liejin Guo

International Research Centre for Renewable Energy, State Key Laboratory of Multiphase Flow in Power Engineering, Xi'an Jiaotong University, Shaanxi 710049, P. R. China.

Email: j.su@mail.xjtu.edu.cn

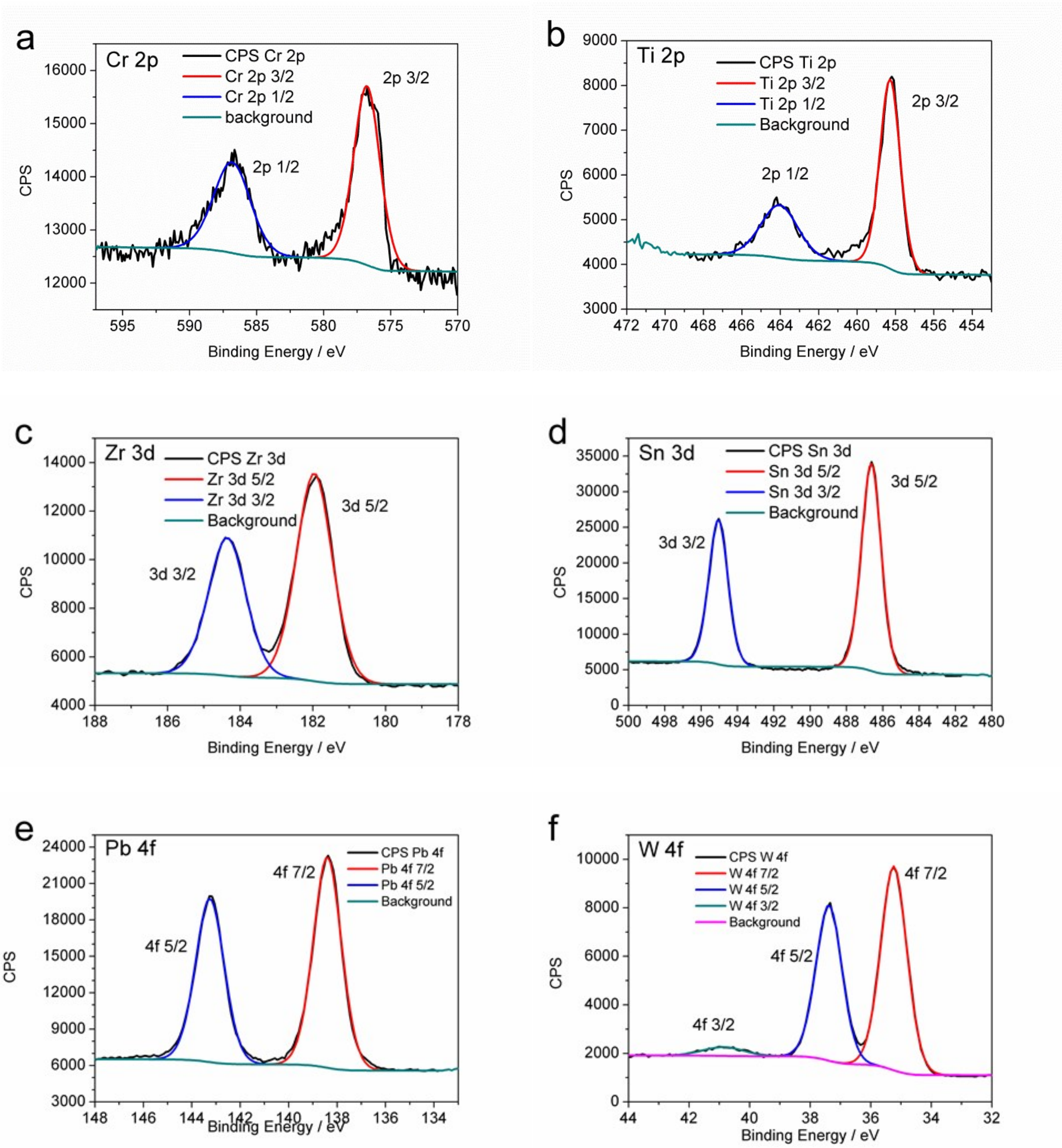

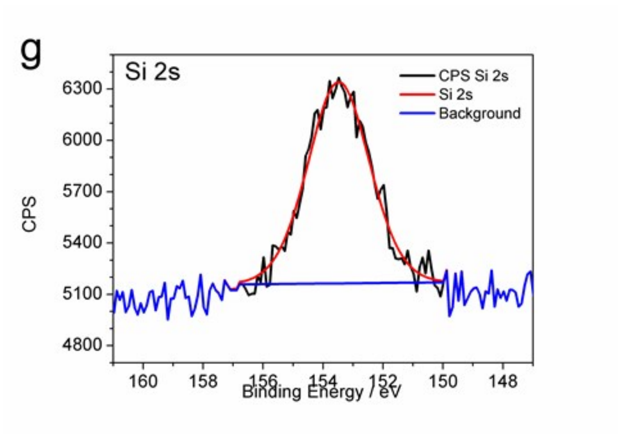

Fig. S1. XPS spectra of various dopant elements

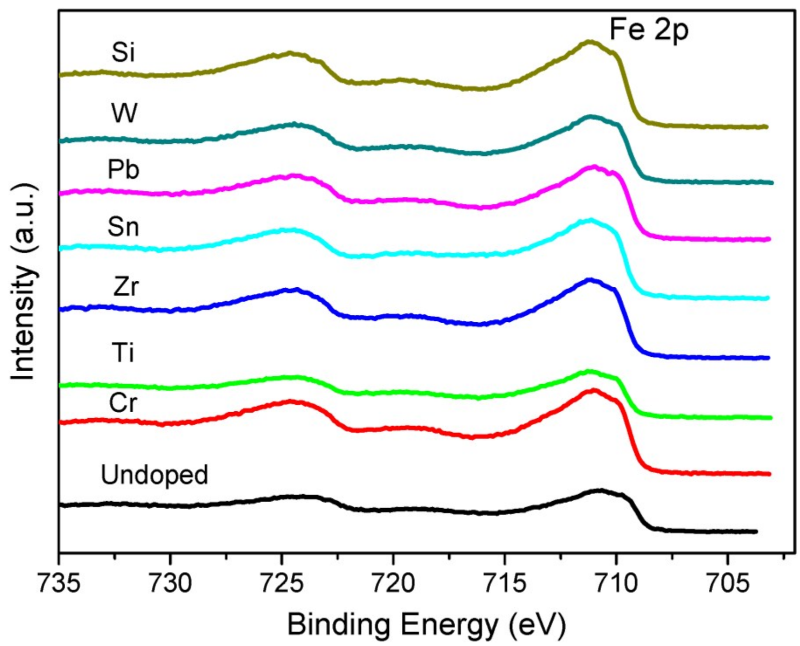

Fig. S2. Fe 2p XPS spectra of bare flat-shaped and various element doped hematite photoelectrodes.

Table S1. Summary of binding energy and corresponding valence states for different elements doped planar hematite photoelectrode

Element	Binding Energy/eV	Valence state
Cr 2p	576.7	+3
Ti 2p	458.3	+4
Zr 3d	182.0	+4
Sn 3d	486.6	+4
Pb 4f	138.4	+2
W 4f	35.2	+6

Si 2p	102.4	+4 (silicates)

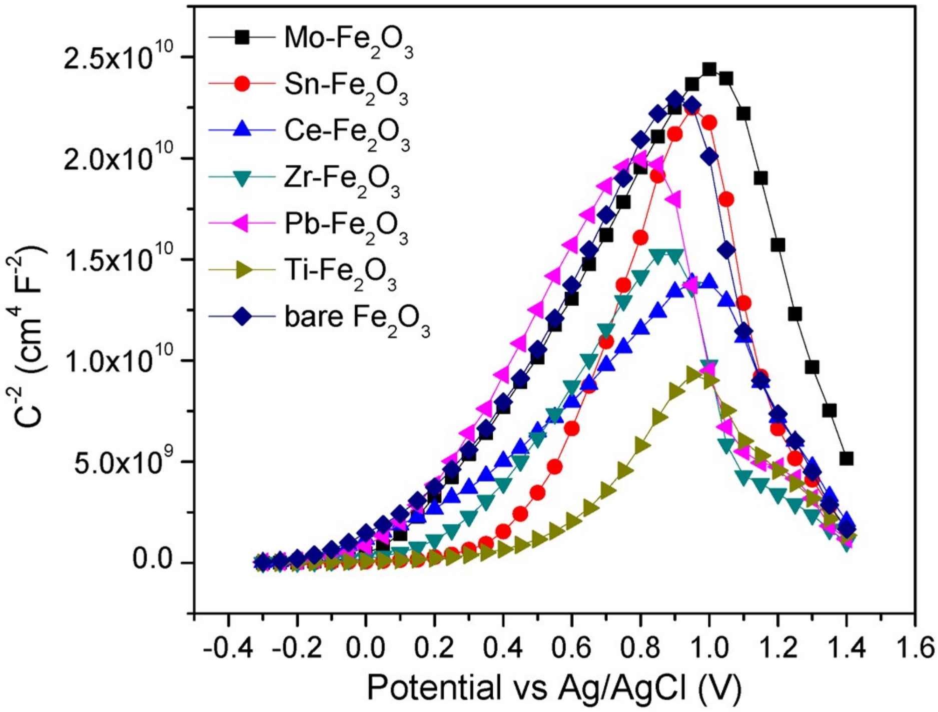

Fig. S3. Mott-Schottky plots of bare and different elements doped hematite nanorod photoelectrodes collected at 977 Hz in the dark.

Table S2 Summary of Parameters derived from Figure S3 and Photocurrent at 1.23V vs Ag/AgCl for bare and different elements doped hematite nanorod photoelectrodes

Element	slope	Flat-band potential (V vs. Ag/AgCl)	N_d (cm^{-3})	Photocurrent $mA\cdot cm^{-2}$
Mo	2.726e10	0.160	6.46565E17	0.0307
Sn	4.788e10	0.464	3.68115E17	0.64841
Ce	1.662e10	0.010	1.06049E18	0.22166
Zr	2.659e10	0.273	6.62857E17	0.94013
Pb	3.099e10	0.110	5.68743E17	0.34395
Ti	2.491e10	0.583	7.07562E17	1.13682
undoped	3.196e10	0.166	5.51482E17	0.05541

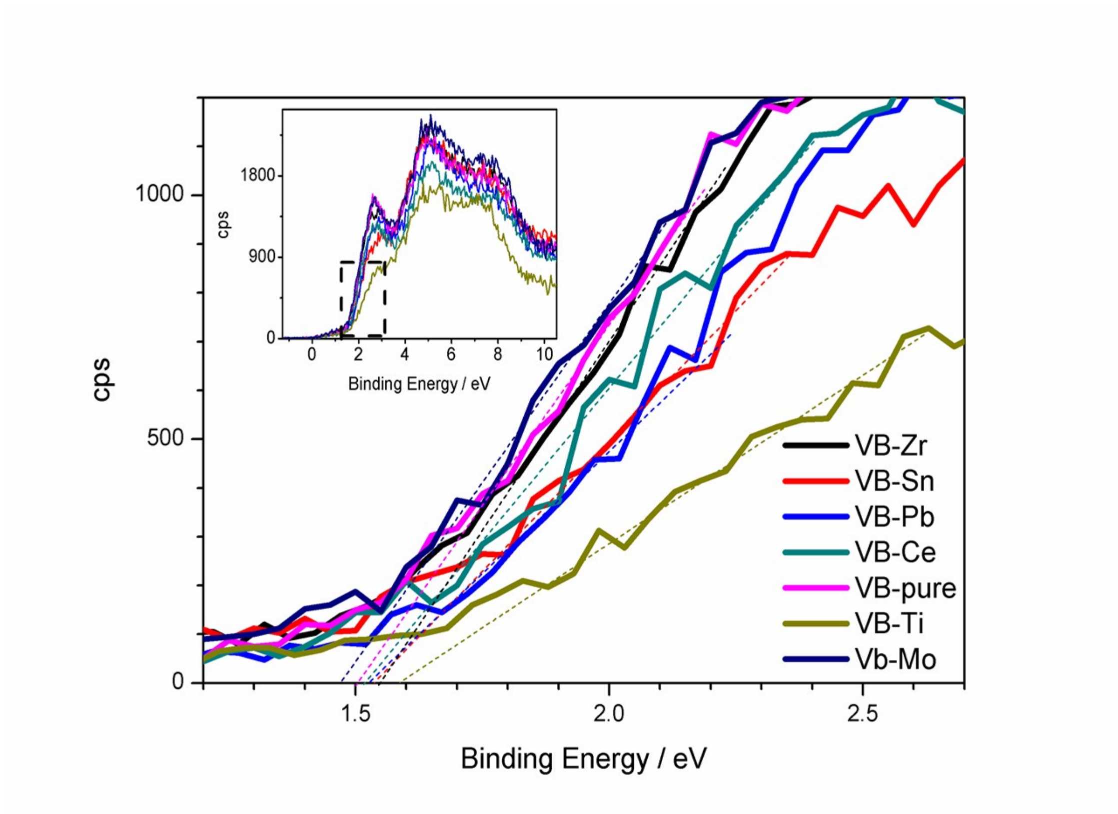

Fig. S4. Valence band spectra of pure and different elements doped hematite nanorod photoelectrodes

Table S3 Summary of Valence Band Maximums for bare and different elements doped hematite nanorod photoelectrodes

Dopant	Valence Band Maximum (eV vs Fermi Level of Equipment)
Ti	1.59
Zr	1.55
Sn	1.54
Pb	1.52
Ce	1.52
Pure	1.50
Mo	1.47